Supporting Information (SI):

V doping Ni_2P nanoparticles grafted g-C_3N_4 nanosheets for enhanced photocatalytic hydrogen evolution performance under visible-light

Qian Chen[a], Jianfeng Huang[a,*], Xiao Ting [a], Liyun Cao[a*], Dinghan Liu[b], Xiaoyi Li[a], Mengfan Niu[a], Guoting Xu[a], Koji Kajiyoshi[c], Liangliang Feng[a,*]

[a] *School of Materials Science & Engineering, International S&T Cooperation Foundation of Shaanxi Province, Shaanxi University of Science and Technology, Xi'an 710021, China.*

[b] *School of Electronic Information and Artificial Intelligence, Shaanxi University of Science and Technology, Xi'an 710021, China.*

[c] *Kochi Key University, Research Laboratory of Hydrothermal Chemistry, Kochi 780-8520, Japan.*

[*] Corresponding authors.

E-mail addresses: huangjf@sust.edu.cn (J. Huang), caoliyun@sust.edu.cn (L. Cao), fengll@sust.edu.cn (L. Feng).

Number of pages: 13

Number of figures: 10

Number of tables: 1

Containing 20 pages, 17 Figures and 1 Tables

Additional images and data:

Figure S1. XRD pattern of NiV-LDH and NiV-LDH/g-C_3N_4.

Figure S2. (a) N_2 adsorption−desorption isotherms at 77 K and (b) the corresponding pore size distribution curves of V-Ni_2P/g-C_3N_4.

Figure S3. SEM images of (a) g-C_3N_4, (b) NiV-LDH, (c) V-Ni_2P; TEM images of (d) g-C_3N_4.

Figure S4. TEM images of (a-b) NiV-LDH (2 μm), (c-d) V-Ni_2P (50 nm).

Figure S5. SEM images of (a) V-Ni_2P/g-C_3N_4, (b) Ni_2P/g-C_3N_4.

Figure S6. TEM images of V-Ni_2P/g-C_3N_4.

Figure S7. The banding energy of pure g-C_3N_4 and 7.8 wt% V-Ni_2P/g-C_3N_4.

Figure S8. (a) SEM and (b) TEM images of V-Ni_2P/g-C_3N_4 after tests.

Figure S9. The XPS spectra of (a) C 1s, (b) N 1s, (c) Ni 2p, (d) P 2p, (e) V 2p for V-Ni_2P/g-C_3N_4 after tests.

Figure S10. The valence band of 7.8 wt% V-Ni_2P/g-C_3N_4.

Table S1. Summary of the Photocatalytic H_2 Evolution on g-C_3N_4-Based Photocatalysts.

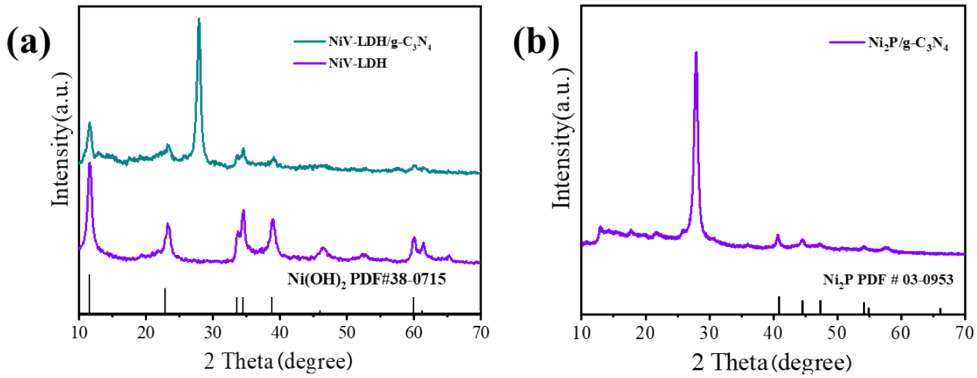

Figure S1. XRD pattern of (a) NiV-LDH and NiV-LDH/g-C_3N_4; (b) Ni_2P/g-C_3N_4

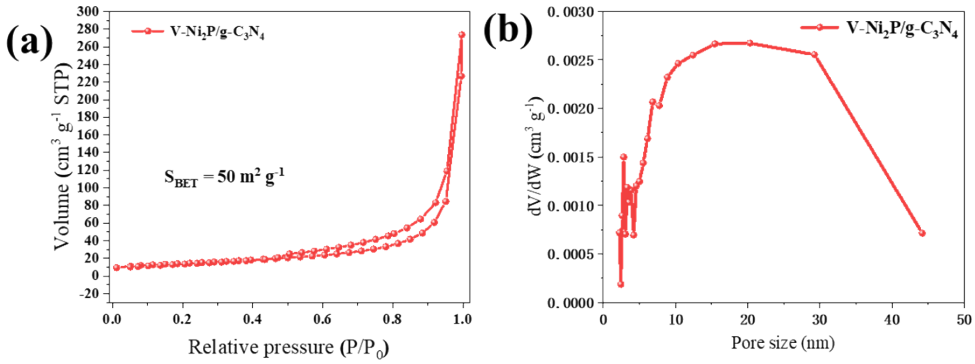

Figure S2. (a) N_2 adsorption−desorption isotherms at 77 K and (b) the corresponding pore size distribution curves of V-Ni_2P/g-C_3N_4.

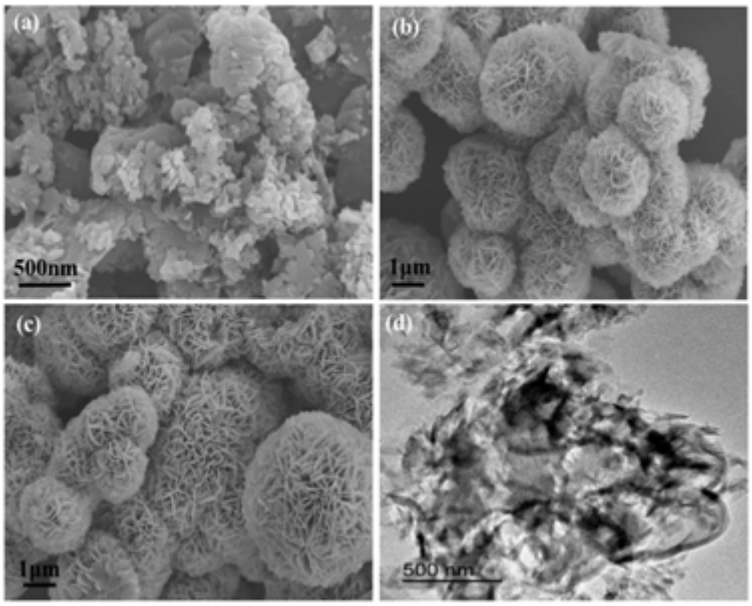

Figure S3. SEM images of (a) g-C_3N_4, (b) NiV-LDH, (c) V-Ni_2P; TEM images of (d) g-C_3N_4.

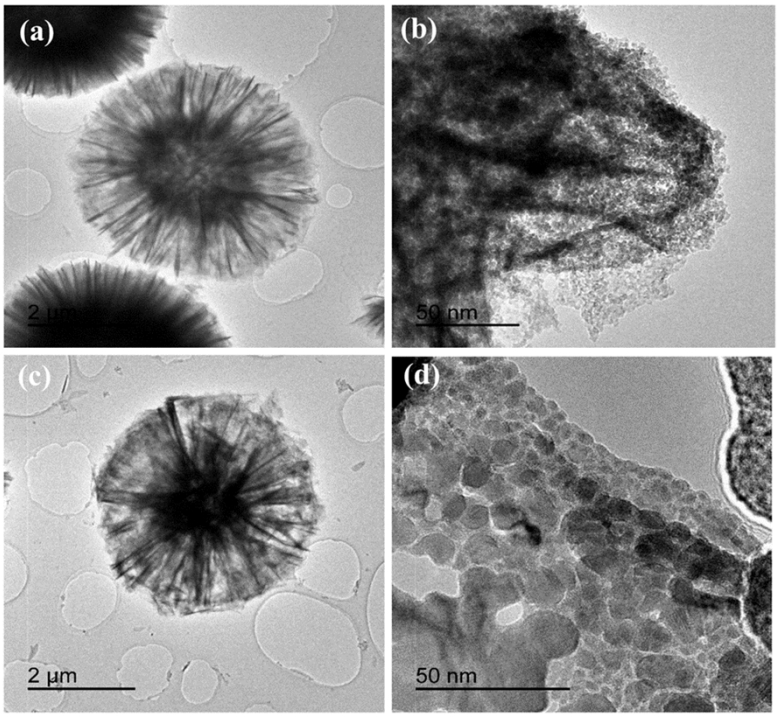

Figure S4. TEM images of (a-b) NiV-LDH (2 μm), (c-d) V-Ni_2P (50 nm).

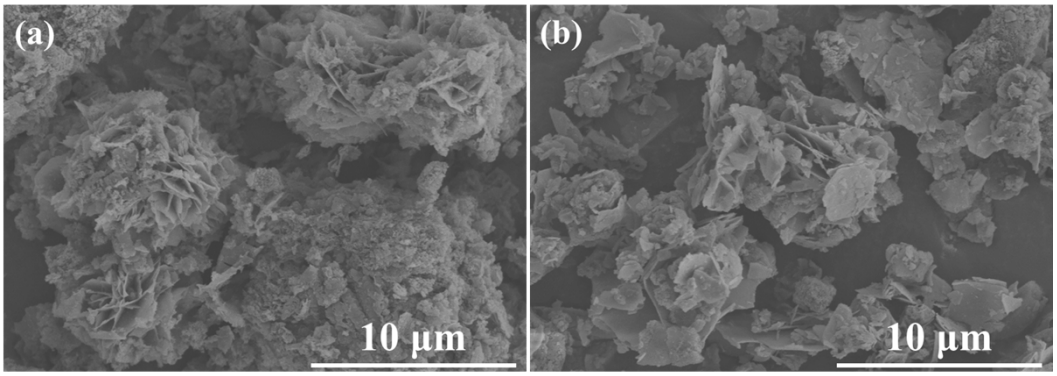

Figure S5. SEM images of (a) V-Ni_2P/g-C_3N_4, (b) Ni_2P/g-C_3N_4.

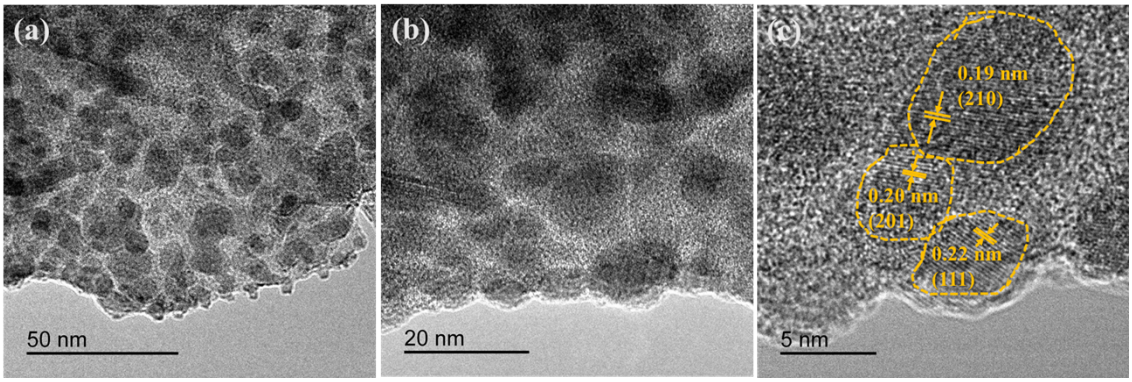

Figure S6. TEM images of V-Ni_2P/g-C_3N_4.

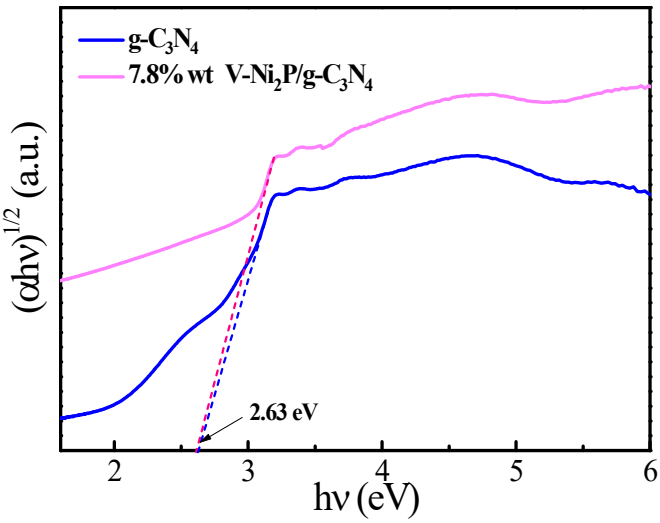

Figure S7. The banding energy of pure g-C_3N_4 and 7.8 wt% V-Ni_2P/g-C_3N_4.

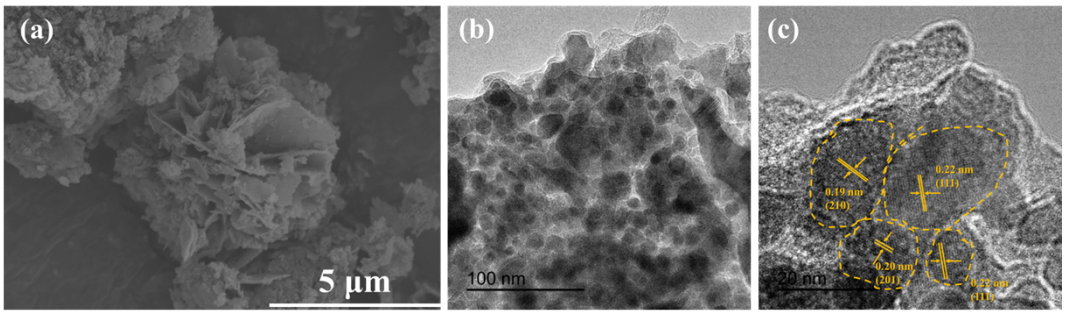

Figure S8. (a) SEM and (b) TEM images of V-Ni_2P/g-C_3N_4 after tests.

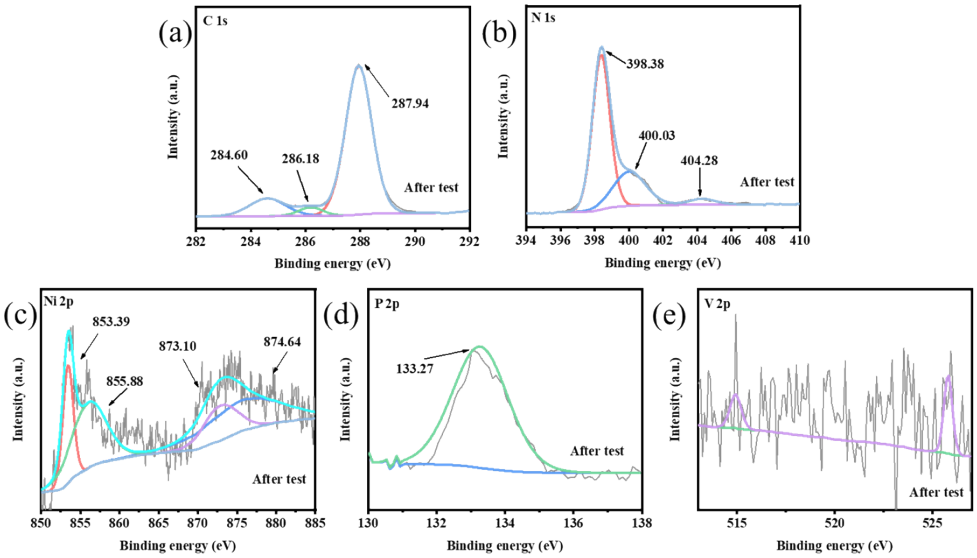

Figure S9. The XPS spectra of (a) C 1s, (b) N 1s, (c) Ni 2p, (d) P 2p, (e) V 2p for V-Ni_2P/g-C_3N_4 after tests.

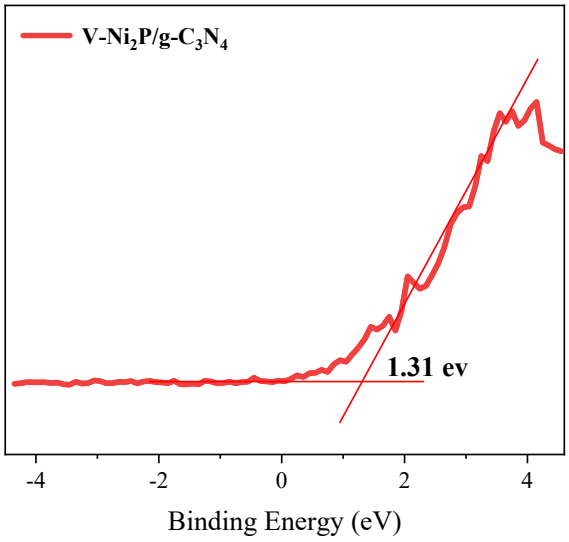

Figure S10. The valence band of pure g-C_3N_4 and 7.8 wt% V-Ni_2P/g-C_3N_4.

Table S1. Summary of the Photocatalytic H_2 Evolution on g-C_3N_4-Based Photocatalysts

	Photocatalysts	Co-catalysts	Power (Xe lamp), wavelength	Activity μmol h^{-1} g^{-1}	Reference
1	**g-C_3N_4**	**V-Ni_2P**	**300 W, λ > 420 nm**	**271.5**	**This work**
2	g-C_3N_4	Co_2P	300 W, λ > 420 nm	128.4	30
3	g-C_3N_4	FeP	300 W, λ > 420 nm	177.9	33
4	g-C_3N_4	MoP	300 W, λ > 420 nm	327.5	39
5	g-C_3N_4	Mo-Mo_2P	300 W, λ > 420 nm	219.7	55
6	g-C_3N_4	CQDs, Pt	400 W, λ > 420 nm	116.1	68
7	g-C_3N_4	$Ni_{12}P_5$	350 W, λ > 400 nm	126.6	69
8	g-C_3N_4	Ni	500 W	168.2	70
9	g-C_3N_4	NiS	150 W, λ > 400 nm	84	71